



HAL
open science

Efficient Plasma Cell Differentiation and Trafficking Require Cxcr4 Desensitization

Vincent Biajoux, Jessica Natt, Christelle Freitas, Nagham Alouche, Antoine Sacquin, Patrice Hemon, Françoise Gaudin, Nicolas Fazilleau, Marion Espeli,
Karl Balabanian

► **To cite this version:**

Vincent Biajoux, Jessica Natt, Christelle Freitas, Nagham Alouche, Antoine Sacquin, et al.. Efficient Plasma Cell Differentiation and Trafficking Require Cxcr4 Desensitization. *Cell Reports*, 2016, 17 (1), pp.193-205. 10.1016/j.celrep.2016.08.068 . inserm-02439879

HAL Id: inserm-02439879

<https://inserm.hal.science/inserm-02439879>

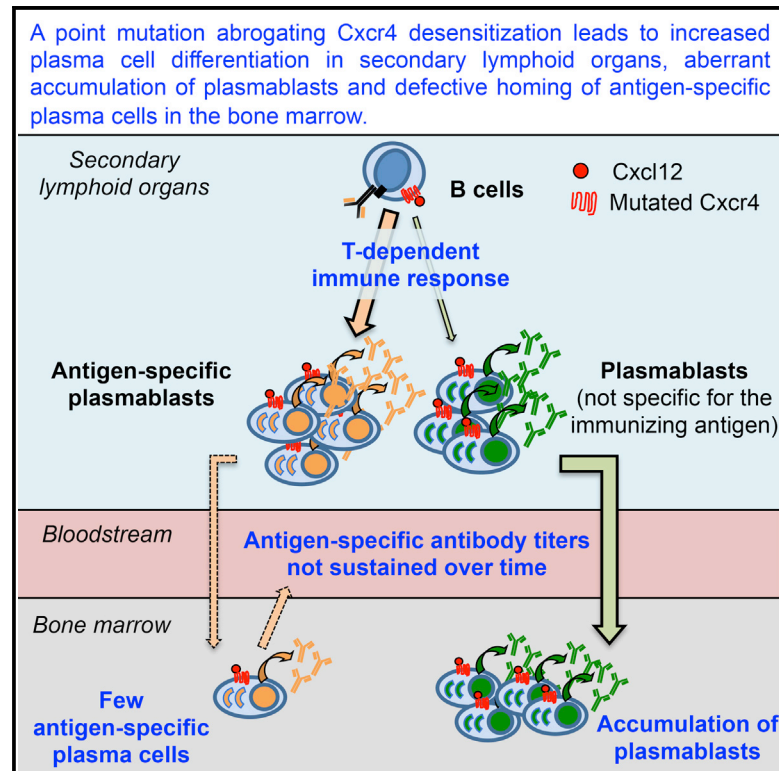
Submitted on 14 Jan 2020

HAL is a multi-disciplinary open access archive for the deposit and dissemination of scientific research documents, whether they are published or not. The documents may come from teaching and research institutions in France or abroad, or from public or private research centers.

L'archive ouverte pluridisciplinaire **HAL**, est destinée au dépôt et à la diffusion de documents scientifiques de niveau recherche, publiés ou non, émanant des établissements d'enseignement et de recherche français ou étrangers, des laboratoires publics ou privés.

Efficient Plasma Cell Differentiation and Trafficking Require Cxcr4 Desensitization

Graphical Abstract



Authors

Vincent Biajoux, Jessica Natt, Christelle Freitas, ..., Nicolas Fazilleau, Marion Espéli, Karl Balabanian

Correspondence

marion.espeli@u-psud.fr (M.E.), karl.balabanian@u-psud.fr (K.B.)

In Brief

Using a mouse model harboring a gain-of-function mutation in *Cxcr4*, Biajoux et al. show that Cxcr4 desensitization is a crucial regulatory mechanism controlling plasma cell differentiation and trafficking. This mutation is associated with an accumulation of plasmablasts in the bone marrow and defective maintenance of serum antibody titers.

Highlights

- Cxcr4 desensitization controls plasma cell differentiation
- Cxcr4 desensitization inhibits plasmablast accumulation in the bone marrow
- Cxcr4 desensitization is required for antigen-specific plasma cell trafficking
- Cxcr4 desensitization is required for maintaining antigen-specific antibody titers



Efficient Plasma Cell Differentiation and Trafficking Require Cxcr4 Desensitization

Vincent Biajoux,^{1,6} Jessica Natt,^{1,6} Christelle Freitas,¹ Nagham Alouche,¹ Antoine Sacquin,^{2,3,4} Patrice Hemon,⁵ Françoise Gaudin,¹ Nicolas Fazilleau,^{2,3,4} Marion Espéli,^{1,*} and Karl Balabanian^{1,7,*}

¹INSERM UMR996 – Inflammation, Chemokines and Immunopathology, Université Paris-Sud and Université Paris-Saclay, Clamart 92140, France

²INSERM U1043, Toulouse 31300, France

³CNRS U5282, Toulouse 31300, France

⁴Centre de Physiopathologie de Toulouse Purpan, Université Toulouse III Paul-Sabatier, Toulouse 31300, France

⁵Plateforme d'Histologie (PHIC), Institut Paris-Saclay d'Innovation Thérapeutique (IPSIT), Clamart 92140, France

⁶Co-first author

⁷Lead Contact

*Correspondence: marion.espeli@u-psud.fr (M.E.), karl.balabanian@u-psud.fr (K.B.)

<http://dx.doi.org/10.1016/j.celrep.2016.08.068>

SUMMARY

CXCR4 plays a central role in B cell immune response, notably by promoting plasma cell (PC) migration and maintenance in the bone marrow (BM). Gain-of-function mutations in *CXCR4* affecting receptor desensitization have been reported in the rare immunodeficiency called WHIM syndrome (WS). Despite lymphopenia, patients mount an immune response but fail to maintain it over time. Using a knockin mouse model phenocopying WS, we showed that, counter-intuitively, a gain of *Cxcr4* function inhibited the maintenance of antibody titers after immunization. Although the *Cxcr4* mutation intrinsically and locally promoted germinal center response and PC differentiation, antigen-specific PCs were barely detected in the BM, a defect mirrored by early accumulation of immature plasmablasts potentially occupying the survival niches for long-lived PCs. Therefore, fine-tuning of *Cxcr4* desensitization is critically required for efficient PC differentiation and maintenance, and absence of such a regulatory process may account for the defective humoral immunity observed in WS patients.

INTRODUCTION

The warts, hypogammaglobulinemia, infections, and myelokathexis syndrome (WS) is a rare combined immuno-hematologic disorder characterized by chronic pan-leukopenia, including circulating B and T lymphocytes (Dotta et al., 2011; Kawai and Malech, 2009). Despite this, patients show limited susceptibility to pathogens, with the notable exception of human papillomavirus and respiratory encapsulated bacteria (Kawai and Malech, 2009). Cellular and humoral immune responses are largely intact after immunization, but oligoclonality, impaired memory B cell function, and vaccination failures have been re-

ported (Gulino et al., 2004; Handisurya et al., 2010; Mc Guire et al., 2010). Together these suggest preserved short-term adaptive immune responses but a defect in the durability of protective memory humoral responses. The mechanisms underlying these defects in adaptive immunity are largely unknown.

An important advance in our understanding of the pathogenesis of the WS was the discovery that most WS cases were associated with a heterozygous gain-of-function mutation in the gene encoding the G-protein-coupled seven-span transmembrane receptor CXCR4, resulting in dysfunction of the signaling axis formed by CXCR4 and its chemokine CXCL12 (Balabanian et al., 2005; Hernandez et al., 2003). This allowed the WS phenotype to be replicated in a knockin mouse model harboring a WS-associated heterozygous mutation in *Cxcr4* (*Cxcr4*⁺¹⁰¹³), causing a distal truncation of the last 15 residues in the carboxyl-terminal tail (C-tail) and resulting in a desensitization-resistant receptor (Balabanian et al., 2012). Mutant mice displayed leukocytes with enhanced migration to Cxcl12 and phenocopied the severe circulating pan-leukopenia. Furthermore, impaired *Cxcr4* desensitization was shown to affect the trafficking of mature lymphocytes between bloodstream and secondary lymphoid organs (LOs) (Balabanian et al., 2012). Indeed, *Cxcr4*⁺¹⁰¹³ mice displayed a splenic follicular hypoplasia without alteration of lymphocyte compartmentalization, whereas their lymph node (LN) architecture was disrupted with an unfurling of the T cell zone within primary B cell follicles. Despite this, serum immunoglobulin M (IgM) and IgG levels were increased in non-manipulated mutant mice compared to their wild-type (WT) littermates, suggesting alterations in the quality and control of the humoral immune response in this model.

Current understanding of the role of Cxcl12 and *Cxcr4* in lymphocyte biology is largely inferred from loss-of-function studies performed using constitutive or conditional mice deficient for *Cxcr4* and *Cxcr4*^{-/-} chimeras (Bannard et al., 2013; Ma et al., 1998; Nie et al., 2004; Tachibana et al., 1998). The Cxcl12/*Cxcr4* pair is thought to regulate the lymphoid trafficking of T cells and orchestrate B cell homing, maturation, and



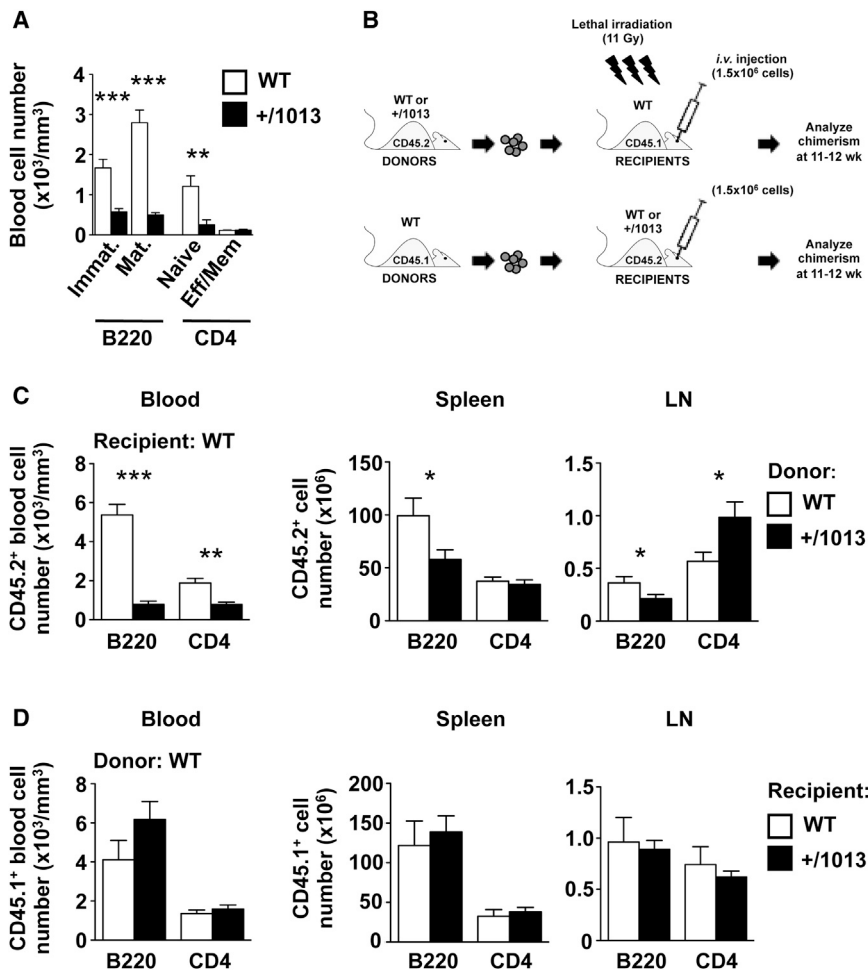


Figure 1. Lymphocyte-Autonomous Defects Lead to Lymphopenia in *Cxcr4*⁺¹⁰¹³ Mice

(A) Quantifications of naive (CD44^{low}CD62L^{high}) and effector/memory (Eff/Mem, CD44^{high}) CD4⁺ T cells, immature (Immat., B220⁺IgM^{high}CD21^{low}) and mature (Mat., B220^{high}IgM^{low}CD21^{high}) B cells were determined from blood samples of WT and *Cxcr4*⁺¹⁰¹³ (+/1013) mice.

(B) Schematic diagram for the generation of BM chimeras.

(C and D) Quantifications of donor CD45.2⁺ (C, WT or +/1013) or CD45.1⁺ (D, WT) CD4⁺ T and B220⁺ B cells recovered from the blood, spleen, and LN of BM chimeras in CD45.1⁺ (C, WT) or CD45.2⁺ (D, WT or +/1013) recipients, respectively. Results are from three independent experiments (mean ± SEM, A: n = 5–9, C and D: n = 5). *p < 0.05, **p < 0.005, and ***p < 0.0005, as compared with WT or donor CD45.2⁺ WT cells. See also Figure S1.

in secondary LOs from *Cxcr4*⁺¹⁰¹³ mice was due to a lymphocyte-intrinsic defect or an alteration of the LO micro-environment. First, BM cells from WT or *Cxcr4*⁺¹⁰¹³ CD45.2⁺ mice were used to reconstitute the hematopoietic compartment of lethally irradiated WT CD45.1⁺ recipients (Figure 1B, top). Eleven weeks after reconstitution, there were significantly lower numbers of CD4⁺ T and B cells in the blood of *Cxcr4*⁺¹⁰¹³ BM-chimeric mice than in those of WT chimeras (Figure 1C, left panel). B cell numbers were also reduced in the spleen and LNs of *Cxcr4*⁺¹⁰¹³ BM-

differentiation in secondary LOs as well as direct plasma cells (PCs) toward specific niches in secondary LOs and bone marrow (BM) (Allen et al., 2004; Bannard et al., 2013; Hargreaves et al., 2001; Nie et al., 2004; Okada et al., 2002; Victora et al., 2010). In this work, we took advantage of our original and relevant *Cxcr4*⁺¹⁰¹³ knockin model to explore the biological impact of a gain-of-function *Cxcr4* mutation on germinal center (GC) formation and primary and memory vaccine responses, as well as on PC differentiation and trafficking.

RESULTS

A Gain of *Cxcr4* Function in B and T Cells Is Sufficient to Induce a Peripheral Lymphopenia

In-depth analysis of the blood compartment in non-manipulated WT and *Cxcr4*⁺¹⁰¹³ mice revealed that mutant mice harbored a severe lymphopenia predominantly affecting naive CD4⁺ T cells and mature recirculating B cells (Figure 1A). Similar to the immunophenotype of WS patients (Gulino et al., 2004), numbers of immature B cells and effector/memory CD4⁺ T cells were less affected. *Cxcr4* is expressed widely, and so we next sought to determine whether this circulating lymphopenia and abnormal lymphocyte compartmentalization

chimeric mice (Figure 1C, middle and right panels). By comparison, as has already been observed in non-manipulated mice (Balabanian et al., 2012), the number of CD4⁺ T cells was comparable in the spleen of both groups of chimeras and was increased in the LNs of *Cxcr4*⁺¹⁰¹³ BM chimeras. Competitive reconstitution experiments in which BM cells from *Cxcr4*⁺¹⁰¹³ CD45.2⁺ mice were mixed at a ratio of 1:1 with WT CD45.1⁺ BM cells and transplanted into lethally irradiated WT CD45.1⁺ recipients confirmed these findings (Figures S1A and S1B). In these mixed chimeras, fewer *Cxcr4*⁺¹⁰¹³ B cells, and to a lesser extent CD4⁺ T cells, were recovered from the blood, spleen, and LNs.

Then, we performed reverse chimeras where CD45.2⁺ WT and *Cxcr4*⁺¹⁰¹³ mice were irradiated and reconstituted with WT CD45.1⁺ BM (Figure 1B, bottom). Here, the numbers of B cells and CD4⁺ T cells were comparable in both experimental groups in blood and LOs (Figure 1D). Finally, we generated chimeras by irradiating sub-lethally μ MT mice, characterized by the almost complete absence of B cells, and then reconstituting them with *Cxcr4*⁺¹⁰¹³ or WT BM (Figure S1C). In these chimeras, the gain-of-function mutation in *Cxcr4* is mostly present in B cells. As expected, *Cxcr4*⁺¹⁰¹³ BM-chimeric mice had normal splenic CD4⁺ T cell counts but a marked splenic B cell lymphopenia

(Figure S1D). Overall, these results indicate that the peripheral B cell lymphopenia observed in *Cxcr4*^{+/-1013} mice results from a cell-intrinsic defect in *Cxcr4*-mediated signaling.

***Cxcr4*^{+/-1013} Mice Mount a Robust Ag-Specific Immune Response Despite Disorganized LN Architecture**

We next sought to determine whether the severe circulating T- and B cell lymphopenia and absence of primary B cell follicles in the LNs impaired the antibody (Ab) response to a thymus-dependent (TD) antigen (Ag). *Cxcr4* signaling in B cells is involved in GC organization and responses (Allen et al., 2004; Bannard et al., 2013), we thus assessed the extent to which the gain-of-function *Cxcr4* mutation affected B cell differentiation and humoral immunity in draining (i.e., inguinal) LNs after subcutaneous immunization with ovalbumin (OVA) emulsified in Sigma adjuvant system (SAS). The TD B cell response was assessed at the peak of the response, 14 days after primary immunization and 5 days after secondary challenge (boost) (Figure 2A). As expected, we detected the formation of peanut agglutinin (PNA)-positive GCs, which are microanatomical sites of B cell expansion, hypermutation, and selection (Liu et al., 1991), after priming and boosting in WT mice. We also observed PNA-positive GCs in mutant mice despite the disorganized architecture of the LNs (Figure 2B). After OVA/SAS priming and boosting, there was a small reduction in total CD19⁺ B cells but a similar number of total GC B cells in LNs from *Cxcr4*^{+/-1013} mice compared to WT mice (Figure 2C, left and middle panels). There was also a significant increase in OVA-specific GC B cell numbers in the LNs of *Cxcr4*^{+/-1013} mice compared to controls (Figure 2C, right panels). As GC B cell formation is dependent on Ag-specific CD4⁺ follicular helper T (Tfh) cells (Vinueza et al., 2005), we investigated whether differences in the Tfh-cell subset could account for this increased representation of OVA-specific GC B cells in mutant mice. In WT and *Cxcr4*^{+/-1013} mice, we found no differences in total CD4⁺ T cells or Tfh cells (CD4⁺/CD44⁺Cxcr5⁺) after both priming and boost (Figure 2D).

We then studied the PC compartment in mutant and WT mice, observing a significant increase in both total and OVA-specific PCs (CD138^{high}B220^{low}) after priming and boost in *Cxcr4*^{+/-1013} mice compared to WT mice (Figure 2E). There was also a greater number of OVA-specific (IgG) antibody-forming cells (AFCs) in the LNs of immunized *Cxcr4*^{+/-1013} mice regardless of the time point as enumerated by ELISpot (Figure 2F). Altogether, these data indicate that the TD B cell response to a protein Ag is enhanced locally in the LNs of *Cxcr4*^{+/-1013} mice.

***Cxcr4*^{+/-1013} Mice Have Increased Ag-Specific PCs Despite Splenic Follicular Hypoplasia**

Contrary to the LNs, the spleen architecture was preserved in *Cxcr4*^{+/-1013} mice; however, the spleen cellularity was much reduced potentially leading to an altered systemic immune response (Balabanian et al., 2012). We therefore immunized WT and *Cxcr4*^{+/-1013} littermates with 4-hydroxy-3-Nitrophenylacetyl-Keyhole Limpet Hemocyanin (NP-KLH) precipitated in aluminum hydroxide (Alum) and then quantified the GC reaction and PC generation at the peak of the response, 9 days after primary immunization and 7 days after a boost with NP-KLH only (Figure 3A). The splenic B cell lymphopenia in *Cxcr4*^{+/-1013} mice

was not corrected upon immunization (Figures 3B and 3C). However, the number of GC B cells was comparable between WT and mutant mice (Figures 3B and 3D, left panel), which suggested that the immune response is normal in *Cxcr4*^{+/-1013} mice despite the B cell lymphopenia. This was particularly obvious when we calculated the ratio of the number of GC B cells to total B cells (Figure 3D, middle panel). Moreover, the number of NP-specific GC B cells was similar between *Cxcr4*^{+/-1013} and WT mice (Figure 3D, right panel). We confirmed this increased ratio of *Cxcr4*^{+/-1013} GC to total B cells by immunostaining spleens harvested 9 days after primary immunization. As shown in Figure 3E, the B cell follicles (stained with an anti-B220 mAb) were smaller in *Cxcr4*^{+/-1013} mice compared to WT littermates, while the GCs (stained with the PNA lectin) were larger, occupying most of the follicles. In line with previous reports (Allen et al., 2004; Bannard et al., 2013), the ratio of dark zone centroblasts (B220⁺FAS^{high}GL7^{high}Cxcr4^{high}CD86^{low}) to light zone centrocytes (B220⁺FAS^{high}GL7^{high}Cxcr4^{low}CD86^{high}) was increased in immunized *Cxcr4*^{+/-1013} mice (Figure 3F). Unlike B cells, there were only marginally fewer CD4⁺ T cells in the spleen of *Cxcr4*^{+/-1013} mice (Figures 3B and 3C) and the numbers of Tfh (CD4⁺PD1^{high}Cxcr5^{high}Foxp3⁻) and follicular regulatory T (Tfr) cells (CD4⁺PD1^{high}Cxcr5^{high}Foxp3⁺) were not significantly different between the mutant and WT mice (Figure 3G), similar to the observation made in LNs.

We then examined the impact of the gain-of-function mutation in *Cxcr4* on PC development. Comparable numbers of PCs were detected in the spleen of both experimental groups (Figure 3H). Quantification of splenic AFCs by ELISpot revealed a clear increase in NP-specific AFCs in immunized *Cxcr4*^{+/-1013} mice regardless of the time point (Figure 3I). Affinity maturation, as assessed by the ratio of high- (NP4) and low- (NP15) affinity NP-specific AFCs, was comparable between WT and *Cxcr4*^{+/-1013} mice (data not shown). We next wondered whether this enhanced PC response was associated with an aberrant retention or localization of PCs in the spleen. As expected (Jacob et al., 1991; Liu et al., 1991), PCs were mostly observed in the bridging channels and the red pulp area of both WT and mutant mice (Figure S2). Of note, PCs in the red pulp of *Cxcr4*^{+/-1013} mice seem more scattered than in WT mice. This could potentially be explained by the reduced follicle size observed in absence of *Cxcr4* desensitization (Figures 3E and S2; Balabanian et al., 2012) and hence the relative expansion of the red pulp in these mutant mice. These findings suggest that the gain of *Cxcr4* function does not lead to aberrant positioning of newly generated PCs in the spleen. Finally, we investigated how the enhanced PC generation observed in absence of *Cxcr4* desensitization affected circulating Ab titers. After a primary immunization, *Cxcr4*^{+/-1013} mice mounted an Ab response against NP similar to that observed in WT mice (Figure 3J). However, this response waned progressively and was not maintained over time to the level observed in WT mice. Similarly, WT and *Cxcr4*^{+/-1013} mice displayed comparable serum titers of OVA-specific IgG after primary subcutaneous OVA immunizations despite the differences in LN OVA-specific PCs (Figures 2E, 2F, and 3K). We also wondered whether this discrepancy between serum titer and splenic AFC number could be caused by a defect in Ab secretion in *Cxcr4*^{+/-1013} AFCs. However, we did not observe any difference

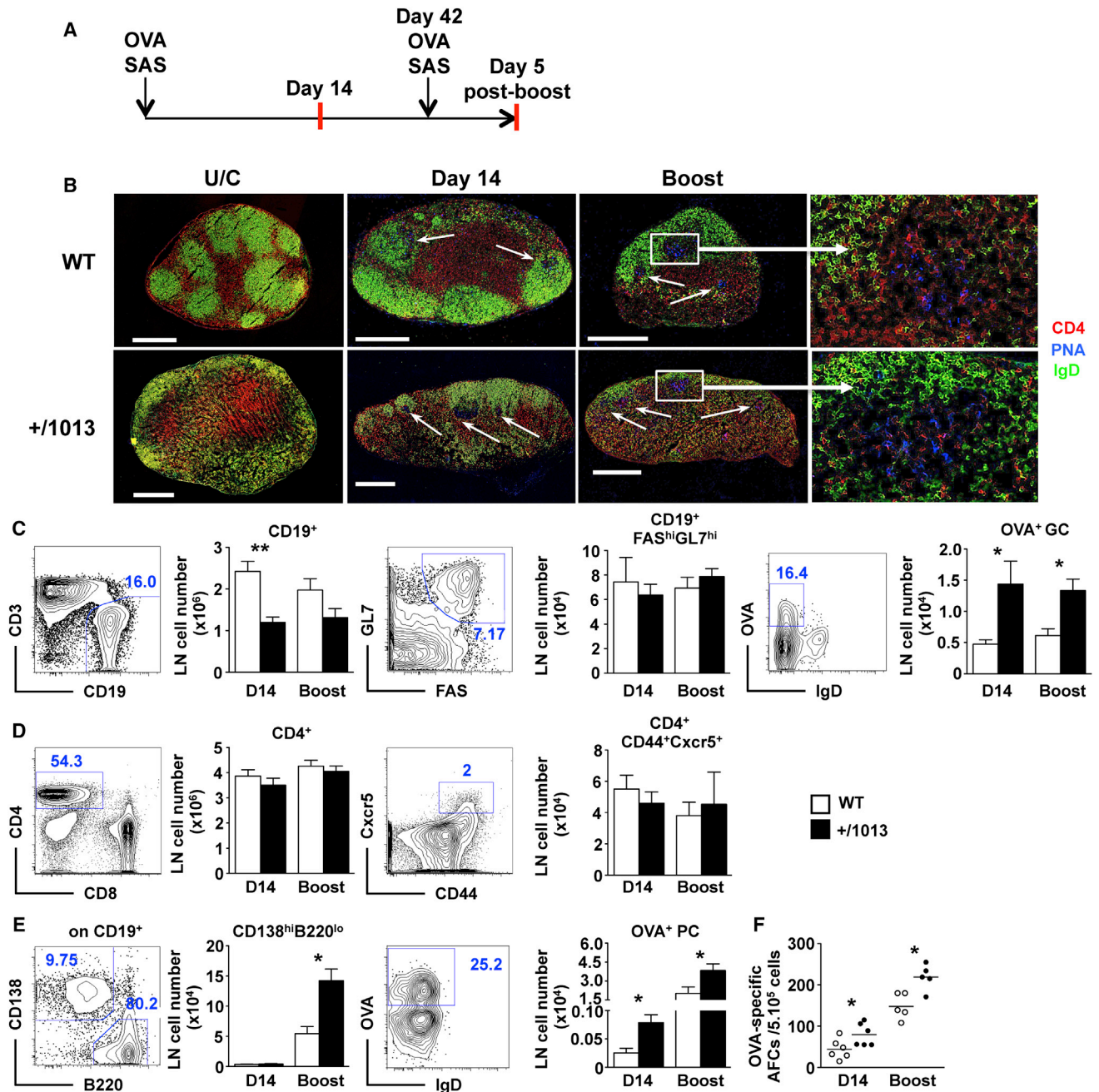


Figure 2. *Cxcr4*⁺¹⁰¹³ Mice Mount a Robust Ag-Specific Immune Response Despite Disorganized LN Architecture

(A) Representative diagram of the immunization protocol and experimental time points.

(B) Draining lymph nodes (LN) sections from WT and *Cxcr4*⁺¹⁰¹³ mice were obtained before immunization (U/C, unchallenged) or after primary (day 14 after challenge) and boost (day 5 after boost) subcutaneous immunizations with adjuvanted OVA and stained for CD4, PNA, and IgD. The color code for mAbs or lectin used is shown. White arrows indicate GC structures. Objective, 10 \times ; scale bars represent 500 μ m.

(C) Representative dot-plots and numbers of B cells (CD19⁺CD3⁺), total (CD19⁺CD138^{hi}FAS^{hi}GL7^{hi}), and OVA-specific (CD19⁺CD138^{hi}FAS^{hi}GL7^{hi}IgD⁺OVA⁺) GC B cells were determined from LNs after priming and boost.

(D) Representative dot plots and numbers of CD4⁺ T cells (CD3⁺B220[−]CD8[−]CD4⁺) and CD44⁺CD62L[−]Cxcr5⁺ Tfh-enriched cell population.

(E) Representative dot plots and numbers of total (CD19⁺B220^{low}CD138^{hi}) and OVA-specific (B220^{low}CD138^{hi}IgD⁺OVA⁺) PCs.

(F) ELISpot assay of OVA-specific (IgG) AFCs in LNs after challenge or boost immunization. Lines indicate the mean and each circles represent the mean value of ELISpot triplicates for one mouse.

Results are from three independent determinations (B) or from three independent experiments (C–F) (mean \pm SEM, n = 5–6). *p < 0.05 and **p < 0.005, as compared with WT cells.

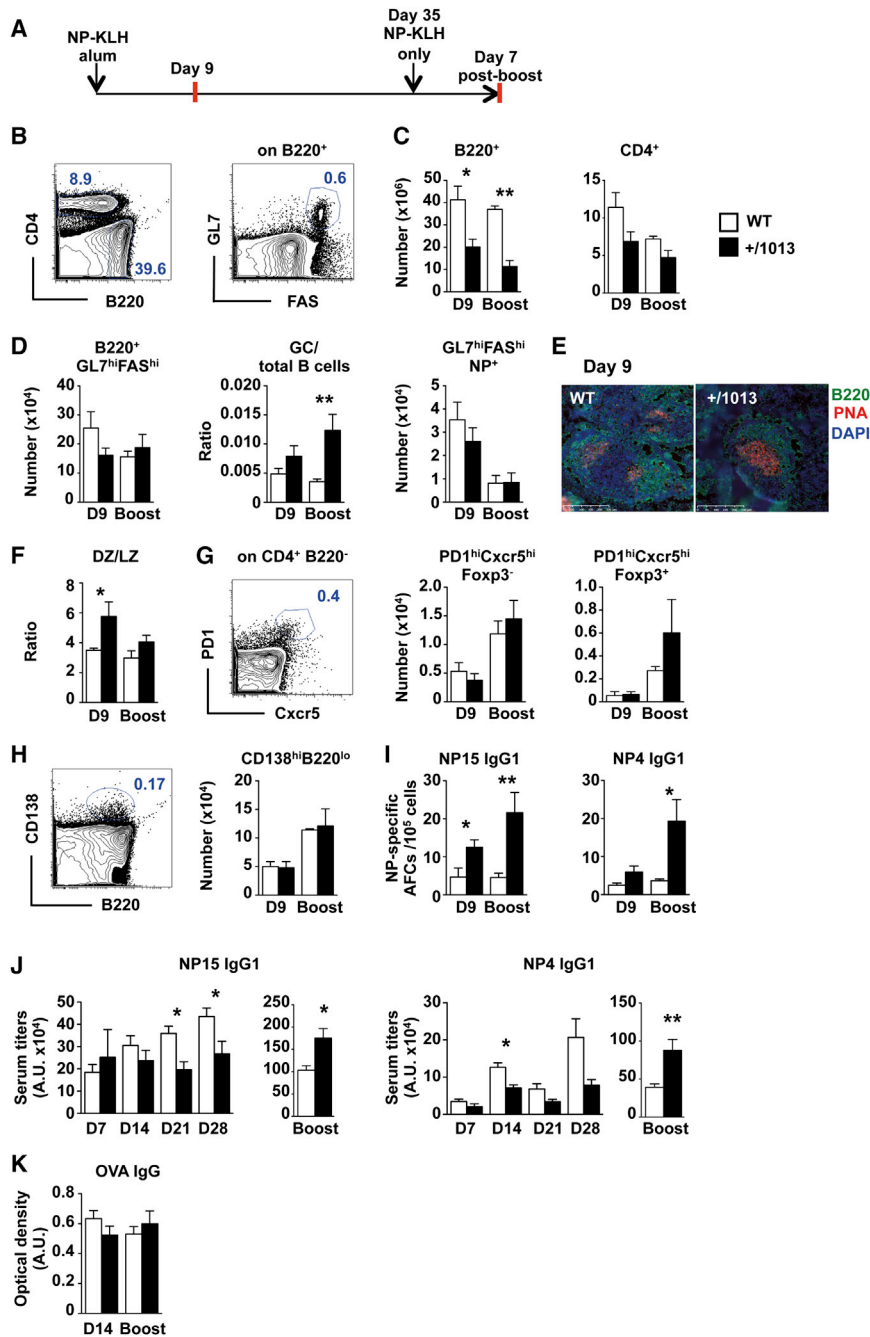


Figure 3. The Gain-of-Cxcr4-Function Mutation Leads to Increased Ag-Specific PC Generation in the Spleen

(A) Representative diagram of the immunization protocol and experimental time points.

(B) Representative dot plots for the gating of B (B220⁺), CD4⁺ T (CD4⁺), and GC B (B220⁺ FAS^{high}GL7^{high}) cells.

(C) Quantification of B and CD4⁺ T cells in the spleen of WT and *Cxcr4*^{+/-1013} mice 9 days (D9) after primary immunization and 7 days after secondary immunization (Boost) with NP-KLH.

(D) Quantification of GC B cells (left panel), ratio of GC B cells over total B cells (middle panel), and NP-specific GC B cells (right panel) in the spleen of WT and *Cxcr4*^{+/-1013} mice.

(E) Representative immunostaining of B cell follicles and GC in the spleen of WT and *Cxcr4*^{+/-1013} mice 9 days after primary immunization. The color code for the mAbs used is shown. Objective, x20; scale bars represent 250 μ m.

(F) Quantification of the ratio of dark zone and light zone GC B cells gated as B220⁺ FAS^{high}GL7^{high}Cxcr4^{high}CD86^{low} and B220⁺FAS^{high}GL7^{high}Cxcr4^{low}CD86^{high}, respectively.

(G) Representative dot plot for the gating of Tfh cells (CD4⁺Cxcr5^{high}PD1^{high}) and quantification of Tfh (CD4⁺Cxcr5^{high}PD1^{high}Foxp3⁻) and Tfr (CD4⁺Cxcr5^{high}PD1^{high}Foxp3⁺) cells in the spleen of WT and *Cxcr4*^{+/-1013} mice.

(H) Representative dot plot for the gating of PCs (CD138^{high}B220^{low}) and quantification of splenic PCs.

(I) Frequencies of NP-specific AFCs of low- and high- (NP15) and high-only (NP4) affinity were determined by ELISpot in the spleen of challenged and boosted mice.

(J) Serum NP-specific Ab titers were determined by ELISA. WT and *Cxcr4*^{+/-1013} mice were bled every week after immunization with NP-KLH. Both low- and high- (NP15, left panels) and high-only (NP4, right panels) affinity NP-specific IgG1 were measured.

(K) Sera from WT and *Cxcr4*^{+/-1013} mice were collected after primary and secondary OVA immunizations and analyzed by ELISA for OVA-specific IgG titers.

AU, arbitrary unit. Results are from three independent experiments (mean \pm SEM, n = 4–6, B–D and F–K) or representative of one out of four independent determinations (E). *p < 0.05 and **p < 0.005, as compared with WT cells. See also [Figures S2 and S3](#).

in spot surface in ELISpot assays ([Figure S3A](#)). As for AFCs, the affinity maturation of circulating NP-specific IgG1 was comparable between WT and mutant mice ([Figure 3J](#)). Mirroring the increased number of NP-specific AFCs observed after boost ([Figure 3I](#)), the serum titers of high- and low-affinity NP-specific IgG1 were increased 7 days after secondary immunization in *Cxcr4*^{+/-1013} mice ([Figure 3J](#)). Moreover, the number of memory B cells defined as B220⁺CD73⁺CD38⁺ was preserved or even increased, respectively, in the spleen and BM of boosted *Cxcr4*^{+/-1013} mice ([Figures S3C and S3D](#)).

Taken together, these findings show that despite splenic follicular hypoplasia, *Cxcr4*^{+/-1013} mice mount an enhanced adaptive immune response compared to WT mice characterized by normal formation of GC B cells, increased production of IgG1 NP-specific AFCs, and a potent memory response after recall. However, in absence of Cxcr4 desensitization, the Ag-specific Ab titers do not reflect the enhanced local immune response observed in the spleen and LNs, and this does not appear to be caused by a defect in Ab secretion or PC mislocalization, nor is dependent on the Ag, the adjuvant or the route of immunization used.

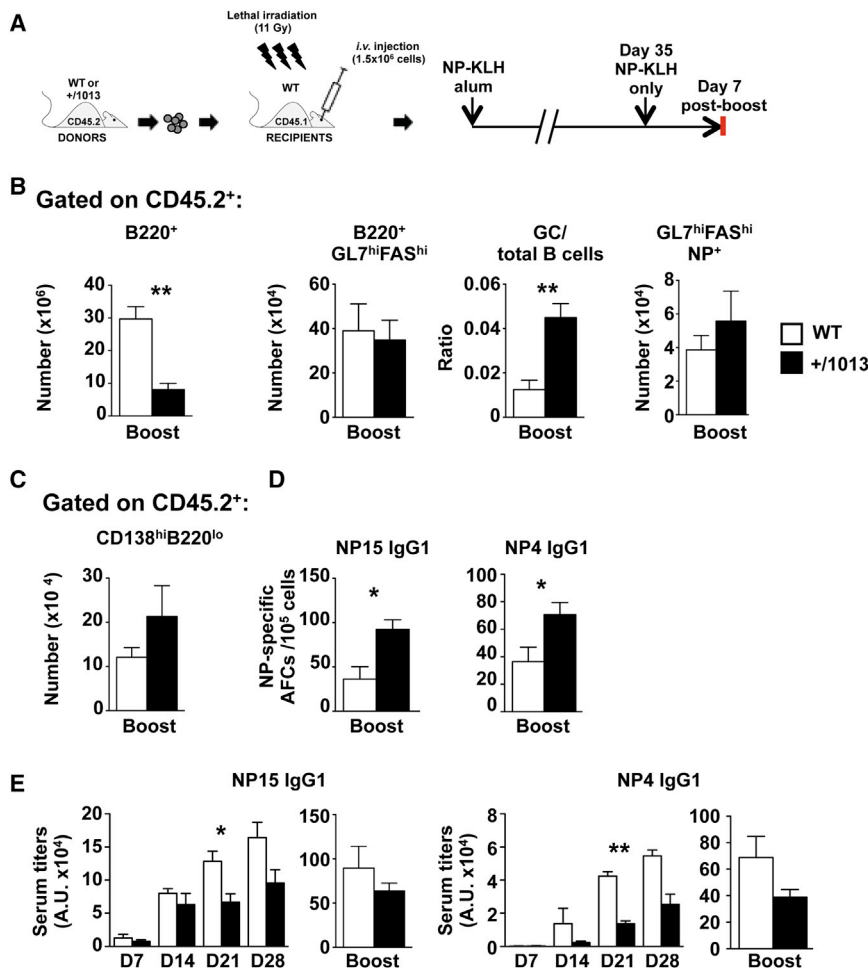


Figure 4. The Deregulation of the Humoral Immunity in *Cxcr4*⁺¹⁰¹³ Mice Is B Cell Autonomous

(A) Representative diagram of the chimera generation, immunization protocol, and experimental time points.

(B) Quantification of CD45.2⁺ total B cells, GC (B220⁺FAS^{high}GL7^{high}) B cells, NP-specific GC B cells, and ratio of GC B cells to total B cells in the spleen of WT and *Cxcr4*⁺¹⁰¹³ BM chimeras 7 days after secondary immunization (boost) with NP-KLH.

(C) Quantification of splenic CD45.2⁺ PCs (B220^{low}CD138^{high}) in boosted WT and *Cxcr4*⁺¹⁰¹³ BM chimeras.

(D) Frequencies of NP-specific AFCs of low- and high- (NP15) and high-only (NP4) affinity were determined by ELISpot in the spleen of boosted chimera mice.

(E) Serum NP-specific Ab titers were determined by ELISA every week after primary immunization and 7 days after boosting with NP-KLH in WT and *Cxcr4*⁺¹⁰¹³ BM chimeras.

Results (mean ± SEM, n = 4–6) are from three independent experiments. *p < 0.05 and **p < 0.005 compared with donor CD45.2⁺ WT cells. See also Figures S1 and S3.

The Deregulation of the Humoral Immunity in *Cxcr4*⁺¹⁰¹³ Mice Is B Cell Autonomous

An important question was whether the enhanced immune response observed in *Cxcr4*⁺¹⁰¹³ mice following TD Ag immunization was intrinsic to a gain of *Cxcr4* function in B cells. We thus generated BM chimeras as in Figure 1B. After reconstitution, mice were immunized with NP-KLH precipitated in Alum and boosted 35 days later with NP-KLH only (Figure 4A). After boosting, the splenic B cell lymphopenia was still observed in mice reconstituted with *Cxcr4*⁺¹⁰¹³ BM (Figure 4B, left panel). Similarly to full mice (Figure 3), the number of GC B cells was unchanged between WT and *Cxcr4*⁺¹⁰¹³ BM chimeras but the ratio of GC B cells to total splenic B cells was significantly increased in *Cxcr4*⁺¹⁰¹³ BM chimeras compared to WT chimeras (Figure 4B, middle panels). The number of NP-specific GC B cells was also comparable between *Cxcr4*⁺¹⁰¹³ and WT BM chimeras (Figure 4B, right panel). The numbers of both Tfh and Tfr cells were identical between the two experimental conditions (data not shown). The total number of PCs was not significantly different (Figure 4C), but NP-specific IgG1 AFCs of both low and high affinity were increased in the spleen of *Cxcr4*⁺¹⁰¹³ BM chimera (Figure 4D). The surface of the spots was equivalent between WT and *Cxcr4*⁺¹⁰¹³ BM chimera (Figure S3B). We also

performed BM chimeras with μ MT mice as recipients and immunized them with NP-KLH (Figures S1C and S1E). In this system, a normal number of GC B cells, an increased ratio of GC B cells to total splenic B cells as well as a slight, albeit not significant, increased number of PCs were observed in immunized *Cxcr4*⁺¹⁰¹³ BM-chimeric mice. These findings indicate that the enhanced PC generation observed in *Cxcr4*⁺¹⁰¹³ mice upon immunization is due to a B cell-intrinsic gain of *Cxcr4* function.

Although the serum titer of NP-specific IgG1 was comparable between experimental groups 7 days after primary immunization, from day 14 it was lower for both low- and high-affinity Abs in *Cxcr4*⁺¹⁰¹³ BM chimeras compared to controls (Figure 4E). Following secondary immunization with NP-KLH only, the *Cxcr4*⁺¹⁰¹³ BM chimeras were able to mount a memory immune response comparable to the one observed in WT BM chimeras (Figure 4E), despite the enhanced number of NP-specific PCs detected in the spleen and the enhanced number of memory B cell observed in the spleen and BM (Figure S3E). Taken together, these findings suggest that *Cxcr4* desensitization is intrinsically required for efficient differentiation or trafficking of long-lived PC.

In Vitro PC Differentiation Is Enhanced in Absence of *Cxcr4* Desensitization

To understand the molecular and cellular mechanisms underlying the increased PC generation in the secondary LOs of *Cxcr4*⁺¹⁰¹³ mice, we first examined the *Cxcl12/Cxcr4* signaling axis. Membrane expression levels of *Cxcr4* were similar between

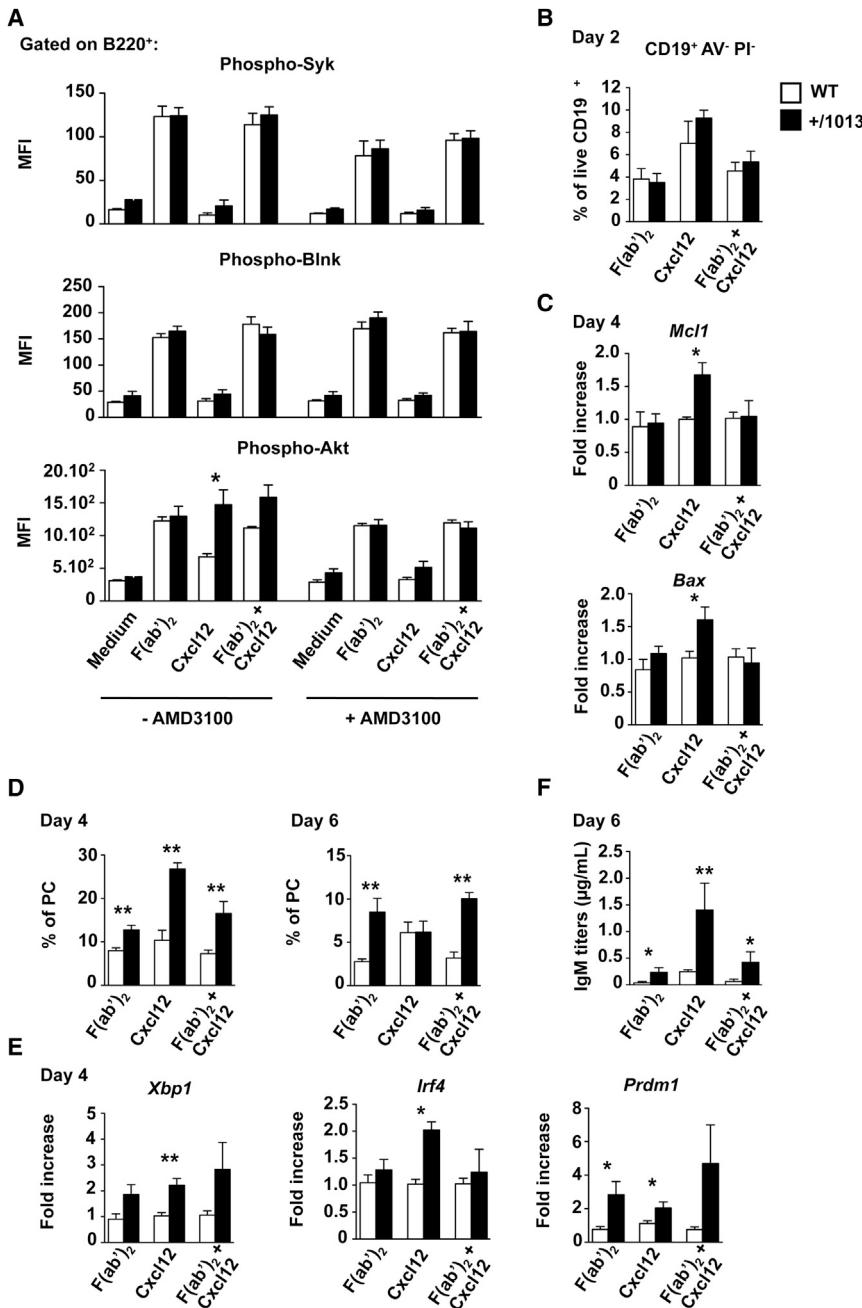


Figure 5. Enhanced Akt Signaling and PC Differentiation in *Cxcr4*⁺¹⁰¹³ B Cells

(A) Splenocytes pre-incubated or not with AMD3100 were stimulated ex vivo with a F(ab)₂ goat anti-mouse IgM and/or Cxcl12 and the mean fluorescence intensity (MFI) of phospho-Syk, -Blnk, and -Akt was determined by flow cytometry. Graphs indicate the MFI of the three phosphoproteins in B220⁺ B cells.

(B) The frequency of live (Annexin V⁻PI⁻) CD19⁺ B cells was determined by flow cytometry after stimulation for 2 days with a F(ab)₂ goat anti-mouse IgM and/or Cxcl12.

(C) Expression levels of *Mcl-1* and *Bax* in splenic B cells stimulated for 4 days with a F(ab)₂ goat anti-mouse IgM and/or Cxcl12 were determined by qRT-PCR. Expression levels were normalized to the level of *Actb* transcripts. The fold change compared to WT B cell expression is shown.

(D–F) Splenic WT and *Cxcr4*⁺¹⁰¹³ B cells were cultured with 1 U/ml IL-4 and 5 ng/ml IL-5 and stimulated as in (C). (D) The proportion of PCs was determined after 4 and 6 days of culture by flow cytometry. (E) The expression levels of *Xbp1*, *Irf4* and *Prdm1* were assessed by qRT-PCR after 4 days of culture. (F) IgM concentration in B cell culture supernatants was measured by ELISA after 6 days of culture. Results (mean ± SEM, n = 3 to 6) are from at least two independent experiments. *p < 0.05 and **p < 0.005 compared with WT cells. See also Figure S4.

splenic WT and *Cxcr4*⁺¹⁰¹³ B cells (data not shown), as previously reported (Balabanian et al., 2012). However, *Cxcr4*⁺¹⁰¹³ B cells displayed impaired Cxcl12 stimulation and increased Cxcl12-promoted chemotaxis that was abolished by the specific Cxcr4 antagonist AMD3100 (Figures S4A and S4B). These dysfunctions likely rely on the altered signaling properties of the truncated Cxcr4 receptor as revealed by Erk1/2 phosphorylation kinetics (Figure S4C). In *Cxcr4*⁺¹⁰¹³ B cells, Erk1/2 activation was strongly increased at 1 min and persisted at longer time points, recapitulating and extending observations we made in patient-derived cells

of Akt than their WT counterparts after Cxcl12 stimulation, with and without BCR crosslinking (Figure 5A). This effect was abrogated by pre-incubation with AMD3100. These results suggest that the gain of Cxcr4 function does not modify signaling through the BCR per se but may enhance signaling through a pathway shared by both Cxcr4 and the BCR converging on Akt.

Signaling through Akt promotes cell survival but also plasmablast differentiation in vitro (Calamito et al., 2010; Omori et al., 2006; Pogue et al., 2000; Suzuki et al., 2003). Survival of B cells from WT and *Cxcr4*⁺¹⁰¹³ mice was similar after 2-day culture in the presence of BCR cross-linking, Cxcl12 or both, as measured

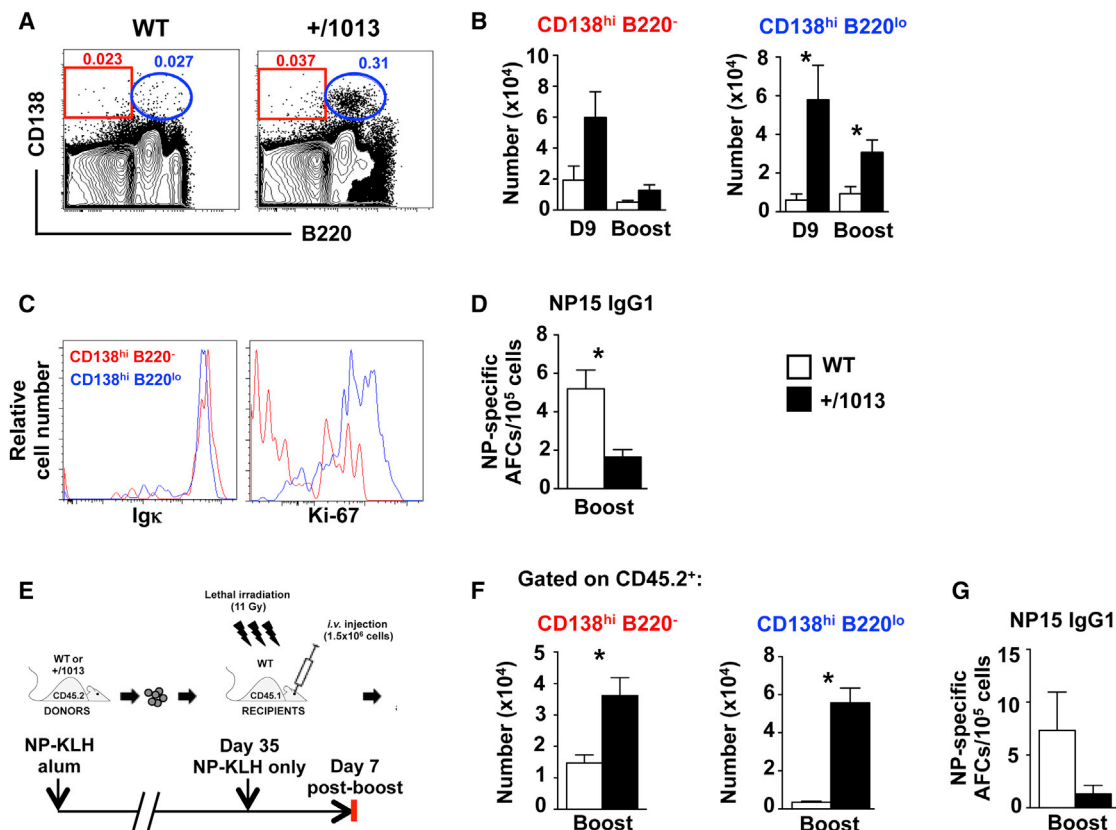


Figure 6. Altered Representation of PCs in the BM of *Cxcr4*⁺¹⁰¹³ Mice

(A) Representative dot plots for the gating of fully differentiated PCs (CD138^{high}B220⁻) and immature PCs (CD138^{high}B220^{low}) in the BM. (B) Quantification of fully differentiated and immature PCs in the BM of WT and *Cxcr4*⁺¹⁰¹³ mice 9 days (D9) after primary immunization and 7 days after secondary immunization (Boost) with NP-KLH. (C) Representative histograms for the expression of intracellular Igκ and Ki-67 in CD138^{high}B220⁻ (red) and CD138^{high}B220^{low} (blue) PCs. (D) Frequency of NP-specific IgG1 AFCs binding to NP with both low and high affinity (NP15) was determined by ELISpot in the BM of boosted mice. (E) Representative diagram of the chimera generation, immunization protocol, and experimental time points. (F) Quantification of CD138^{high}B220⁻ and CD138^{high}B220^{low} cells in the BM of boosted WT and *Cxcr4*⁺¹⁰¹³ BM chimeras. (G) Frequency of NP-specific IgG1 AFCs binding to NP with both low and high affinity (NP15) was determined by ELISpot in the BM of WT and *Cxcr4*⁺¹⁰¹³ BM chimera mice 7 days after secondary immunization (Boost) with NP-KLH. Results are from three independent experiments (mean ± SEM, n = 6, B, D, F, and G) or representative of one experiment out of six independent determinations (A and C). *p < 0.05 compared with WT or donor CD45.2⁺ WT cells. See also Figure S5.

by the frequency of Annexin V⁻ and Propidium Iodide⁻ B cells (Figure 5B). Furthermore, there was no imbalance in the expression of the pro-survival (*Mcl1*) and pro-apoptotic (*Bax*) factors after a 4-day culture (Figure 5C), arguing against a significant effect of the gain of *Cxcr4* function on the survival of B cells in vitro. Finally, we studied the effect of a gain-of-function *Cxcr4* mutation on plasmablast differentiation in vitro. Splenic B cells were cultured for up to 6 days in presence of a BCR cross-linking Ab, Cxcl12 or both. The percentage of plasmablasts was significantly increased at day 4 in all conditions in *Cxcr4*⁺¹⁰¹³ B cells compared to WT cells (Figure 5D). At day 6, there were more *Cxcr4*⁺¹⁰¹³ plasmablasts only in the presence of BCR cross-linking. In line with the results at day 4, expression levels of PC transcriptional regulators, such as *Xbp1*, *Irf4*, and *Prdm1*, were increased in *Cxcr4*⁺¹⁰¹³ compared to WT B cells (Figure 5E). We also detected increased IgM levels in the supernatants of *Cxcr4*⁺¹⁰¹³ B cells cultured for 6 days (Figure 5F). Altogether,

these results show that upon Cxcl12 exposure, the gain-of-*Cxcr4*-function mutation leads to increased Akt signaling in B cells and promotes PC differentiation.

Ag-Specific PCs Are Dramatically Reduced in the BM of *Cxcr4*⁺¹⁰¹³ Mice

Following their generation in secondary LOs, some PCs migrate to the BM where they fully differentiate into long-lived PCs (Radbruch et al., 2006). The BM homing of PCs is thought to rely at least in part on the interaction between *Cxcr4* and its ligand Cxcl12, which is expressed on BM stromal cells (Hargreaves et al., 2001; Sugiyama et al., 2006). We thus reasoned that a gain-of-function mutation in *Cxcr4* might enhance PC trafficking to the BM. In support of this, we observed a slight increase in the number of total PCs (CD138^{high}B220⁻) in the BM of *Cxcr4*⁺¹⁰¹³ mice compared to WT littermates (Figures 6A–6C). However, 7 days after a boost, NP-specific AFCs were barely detectable

in the BM of *Cxcr4*^{+/-1013} mice, while clearly present in the BM of WT mice (Figure 6D). Instead, the BM of mutant but not of WT mice contained a population of cells expressing CD138 and low levels of B220 (Figures 6A and 6B), a phenotype more usually seen on splenic immature PCs (Figure 3H; Kallies et al., 2004). To confirm that these CD138^{high}B220^{low} cells were indeed immature PCs, we showed that they had high levels of intracellular Igκ (Figure 6C, left panel) and that contrary to fully differentiated PCs, they also expressed high levels of Ki-67 (Figure 6C, right panel), indicating that they were still in cycle. A similar result was observed in the BM of immunized *Cxcr4*^{+/-1013} BM chimera with barely detectable NP-specific IgG1 AFCs, increased number of total PCs, and the presence of the same aberrant population of immature PCs (Figures 6E–6G). We wondered whether this altered representation was caused by a change in PC survival within the BM, a process that was reported to be under the control of TRAIL-dependent apoptosis (Ursini-Siegel et al., 2002). However, no difference in the expression of *Trail* was observed in WT and mutant BM (Figure S5A). Cytokines including interleukin-6 (IL-6), BAFF, and APRIL expressed in the BM notably by eosinophils were also shown to modulate PC persistence (Chu et al., 2011; Winter et al., 2010). Expression levels of these cytokines as well as the absolute number of eosinophils and APRIL⁺ eosinophils were similar in WT and mutant mice (Figures S5A–S5D). Thus, enhanced Ag-specific PC generation in the spleen does not translate into increased Ag-specific PCs in the BM, which may explain the defective maintenance of protective Ab titers over time. Furthermore, an aberrant population of immature PCs accumulates in the BM in absence of *Cxcr4* desensitization, potentially impacting the homing or maintenance of Ag specific long-lived PCs.

Cxcr4 Desensitization Prevents the Accumulation of Immature PCs in the BM

Aforementioned findings prompted us to assess the kinetics of generation and appearance of immature PCs and NP-specific AFCs in the spleen and BM of *Cxcr4*^{+/-1013} mice. To this end, WT and *Cxcr4*^{+/-1013} mice were immunized intraperitoneally with NP-KLH in alum and sacrificed at days 3, 6, 9, and 18 (Figure 7A). As previously shown, the number of total B cells was reduced in the spleen of *Cxcr4*^{+/-1013} mice compared to control at all time points analyzed (Figure 7B). In line with this profound splenic hypoplasia, the total number of GC B cells was also reduced in mutant mice (Figure 7C), although their frequency and kinetic of formation were normal (Figure 7D). Finally, the ratio of GC B cells/B cells increased over time and from day 9 was higher in absence of *Cxcr4* desensitization (Figure 7E). Altogether, these results suggest that despite the lymphopenia, the GC form normally in the spleen of the mutant mice. At day 3, the number of total PCs increased transiently in the spleen of *Cxcr4*^{+/-1013} mice (Figure 7F). Strikingly, immature PCs were detected in the BM of mutant mice from day 3 post-immunization, their number increasing until day 9 before slightly decreasing at day 18 (Figure 7G). The number of fully differentiated PCs was starting to increase from day 6 in the BM of *Cxcr4*^{+/-1013} mice (Figure 7H). Finally, we evaluated the generation of Ag-specific AFCs by ELISpot and confirmed enhanced detection of NP-specific IgG1 AFCs in the spleen of *Cxcr4*^{+/-1013} mice at day 9 (Figure 7I).

In contrast, such cells were barely detectable in the BM of mutant mice at all time points tested (Figure 7J), arguing against a delayed homing to the BM. Therefore, in absence of *Cxcr4* desensitization, immature PCs may accumulate very early after primary immunization in the BM, while Ag-specific PCs that are generated later fail to home and persist in this tissue.

DISCUSSION

CXCR4 is known to play an important role in the regulation of B cell homeostasis and activation. However, most of our current knowledge is based on loss-of-function studies using genetic mouse models or pharmacological inhibitors (Beck et al., 2014; Ma et al., 1998, 1999; Nie et al., 2004). In this study, we investigated the role of *Cxcr4* on the B cell response to TD Ags using a unique mouse model with a naturally occurring heterozygous gain-of-function mutation (*Cxcr4*^{+/-1013}). We report that increased *Cxcr4* signaling promotes B cell activation and differentiation but interestingly does not facilitate the generation of long-term Ab titers against TD Ags. Despite a marked peripheral B cell lymphopenia and distorted LN architecture, immunized *Cxcr4*^{+/-1013} mice displayed increased frequency and number of Ag-specific PCs in the spleen and LNs irrespective of the Ag, the adjuvant or the route of immunization used. This may rely partly on enhanced *Cxcr4*-mediated signaling through Akt and increased PC differentiation. However, and counter-intuitively, Ag-specific PCs failed to accumulate in the BM and Ag-specific serum Ab titers were not maintained over time. Long-term BM chimera experiments confirmed the B cell intrinsic nature of the identified defects.

Splenic architecture was not affected by the gain of *Cxcr4* function, but the size and number of the lymphoid follicles were greatly reduced (Balabanian et al., 2012). Despite this profound hypoplasia, surprisingly the number of GC B cells was normal in the immunized mutant mice. *Cxcr4* is pivotal for centroblast localization in the dark zone (Allen et al., 2004; Bannard et al., 2013), where *Cxcl12*-expressing reticular cells have been recently identified (Rodda et al., 2015). Accordingly, we observed an increased centroblast/centrocyte ratio in the spleen of immunized *Cxcr4*^{+/-1013} mice. Although GC B cells can proliferate in both light and dark zones (Bannard et al., 2013), dark zone centroblasts divide more rapidly than centrocytes (Gitlin et al., 2014; Victora et al., 2010), and proliferation is partly impaired in *Cxcr4*-deficient GC B cells (Bannard et al., 2013). One can speculate that a minor increase in the proliferation rate of *Cxcr4*^{+/-1013} GC B cells in the dark zone might account for the normalization of their number compared to WT cells. Despite the enhanced centroblast/centrocyte ratio in *Cxcr4*^{+/-1013} mice, affinity maturation was normal implying that selection of high-affinity clones was not altered (Gitlin et al., 2014, 2015). In line with this, Tfh and Tfr numbers were unchanged in the spleen and LNs of the mutant mice compared to WT littermates, although their function has not been formally assessed. Upon secondary challenge with a TD Ag, memory B cells are thought to respond rapidly and differentiate into plasmablasts (Ochsenbein et al., 2000). Our data suggest this process occurs efficiently in *Cxcr4*^{+/-1013} mice as we observed normal and increased numbers of memory B cells in the spleen and BM respectively. Moreover, increased

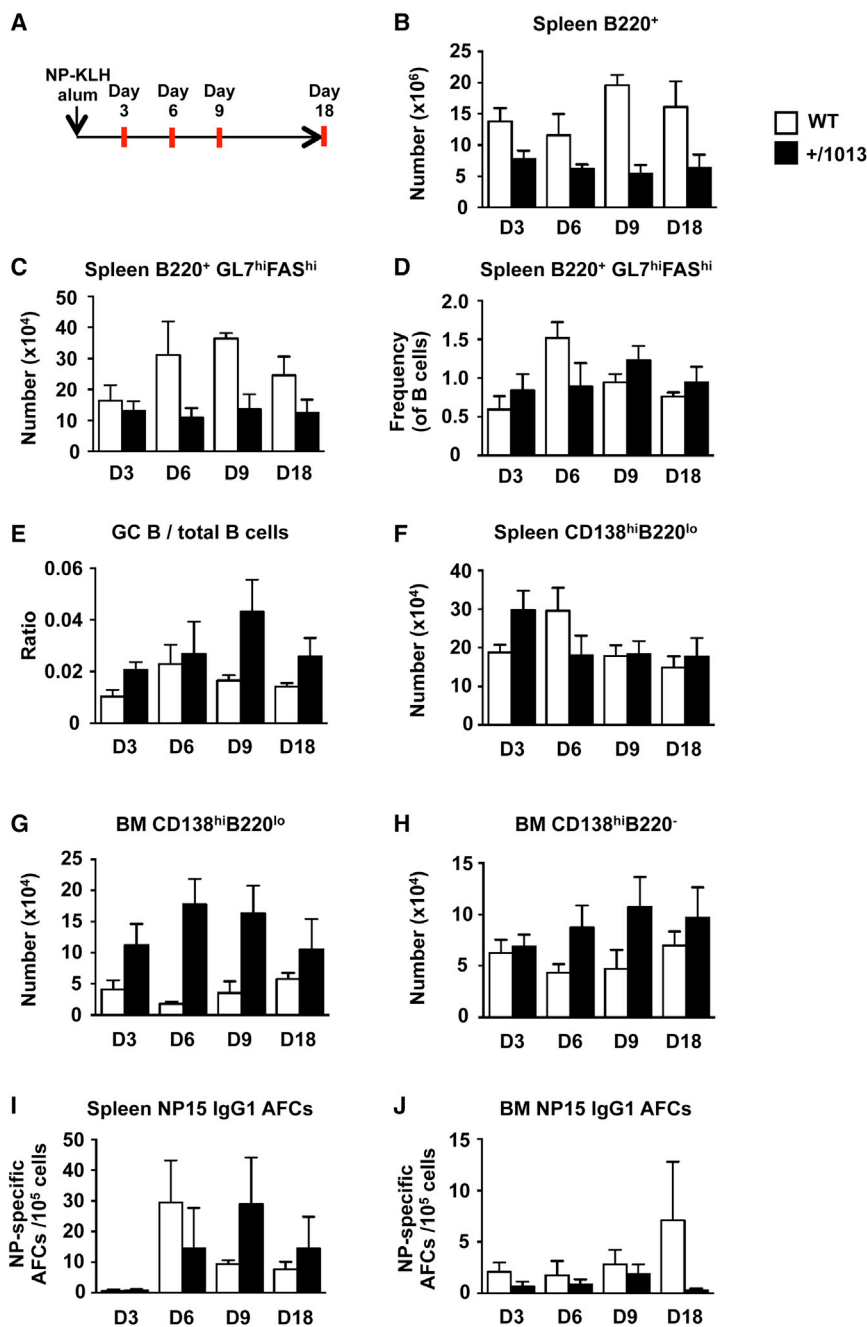


Figure 7. Kinetics of Generation and Appearance of PCs in the Spleen and BM of *Cxcr4*^{+/-1013} Mice

(A) Representative diagram of the immunization protocol and experimental time points.

(B and C) Quantification of total B cells (B220⁺, B) and GC B cells (B220⁺FAS^{high}GL7^{high}, C) in the spleen of WT and *Cxcr4*^{+/-1013} mice 3 (D3), 6 (D6), 9 (D9), and 18 (D18) days after primary immunization with NP-KLH.

(D and E) Frequency of GC B cells among total B cells (D) and ratio of GC B cells over total B cells (E) in the spleen of immunized WT and *Cxcr4*^{+/-1013} mice.

(F) Quantification of PCs (CD138^{high}B220^{low}) in the spleen of immunized WT and *Cxcr4*^{+/-1013} mice.

(G and H) Quantification of immature PCs (CD138^{high}B220^{low}, G) and fully differentiated PCs (CD138^{high}B220⁺, H) in the BM of immunized WT and *Cxcr4*^{+/-1013} mice.

(I and J) Frequencies of NP-specific IgG1 AFCs of low and high (NP15) affinity were determined by ELISpot in the spleen (I) and BM (J) of immunized mice.

Results (mean ± SEM, n ≥ 3) are representative of one out of two (I and J) or three (B–H) independent experiments.

that the capacity of *Cxcr4*^{+/-1013} PCs to secrete Ab was preserved. Supporting this, we found in vitro that Cxcl12 with or without BCR cross-linking enhanced PC differentiation of splenic *Cxcr4*^{+/-1013} B cells and that this was associated with production and secretion of Abs. However, enhanced differentiation of PCs in secondary LOs did not translate in an increased level of circulating NP-specific Abs, and this was even associated with a progressive decrease of specific Ab titer over time.

The defect in circulating Ab could be explained by the strong reduction in NP-specific PCs observed in the BM of immunized *Cxcr4*^{+/-1013} mice. It appears that in absence of *Cxcr4* desensitization and despite the increase in total PCs in the BM, newly generated Ag-specific PCs fail to reach the BM of *Cxcr4*^{+/-1013}

splenic NP-specific AFC numbers and serum titers of high- and low-affinity NP-specific IgG1 were observed 1 week after boosting with NP-KLH alone.

Mechanistically, we showed that *Cxcr4* signaling, together with cross-linking of the BCR, promotes the phosphorylation of Akt in B cells from *Cxcr4*^{+/-1013} mice, and this may account for the enhanced PC number and in vitro differentiation we observed (Omori et al., 2006; Suzuki et al., 2003). Quantification of splenic or LN AFCs by ELISpot revealed an increase in Ag-specific AFCs in immunized *Cxcr4*^{+/-1013} mice regardless of the time point and without a detectable difference in spot size, thus suggesting

mice. One question arising from our findings pertains to the mechanism underpinning defective detection of NP-specific PCs in the BM of mutant mice. Several overlapping possibilities could explain this. First, PCs generated in the spleen and LN of *Cxcr4*^{+/-1013} mice may fail to differentiate into long-term PCs, thus explaining the rapid decrease in NP-specific Ab titers. Somewhat against this hypothesis is the fact that the number of fully differentiated PCs in the BM is normal or even increased at different time points after primary and secondary immunizations. Second, NP-specific PCs may be unable to effectively egress from secondary LOs. Indeed, *Cxcr4* is involved in B cell

and PC entry to and retention within the spleen red pulp and LN medulla, which are both reported to express Cxcl12 (Hargreaves et al., 2001; Nakai et al., 2014; Nie et al., 2004). As such, the gain of Cxcr4 function might lead to an aberrant retention of newly generated PCs in the LN and the spleen. However, our findings do not support this hypothesis as PC localization in the spleen was normal and PCs did not accumulate in this organ with time. Third, the gain of Cxcr4 function may alter the homing of NP-specific PCs to the BM. Cxcr4 is known to participate in the homing of newly generated PCs to the BM (Hargreaves et al., 2001; Hauser et al., 2002). A fraction of these PCs are retained and differentiate into fully mature PCs that survive for long periods of time in highly specialized niches that are not yet fully defined. Our results suggest that some *Cxcr4*⁺¹⁰¹³ PCs are able to migrate to the BM as we found a slight increased number of long-lived PC in the BM of mutant mice. Under-representation of Ag-specific PCs in the BM was observed from day 3 to day 18 after primary immunization and 3 months after boost (data not shown), thus ruling out a delay in BM migration of *Cxcr4*⁺¹⁰¹³ NP-specific PCs from the periphery. Our findings further suggest that the altered representation of NP-specific PCs is unlikely to be caused by defects in cytokine production or cellular sources in the BM. Finally, we identified an unusual population of PCs displaying an immature, highly proliferative phenotype similar to that of splenic plasmablasts that abnormally accumulate very rapidly in the BM of immunized mutant mice. These cells may occupy BM niches normally dedicated to GC-derived Ag-specific PCs. Consequently the lodging of Ag-specific PCs could be altered due to mis-localization in the BM and subsequent lack of appropriate survival and nursing signals required for their maturation and maintenance. Altogether, our results support a model where Cxcr4 desensitization is a critical mechanism controlling which PCs home and persist within the BM.

Mice deficient for the gene encoding the transcription factor *c-Myb* display a similar phenotype to the one of *Cxcr4*⁺¹⁰¹³ mice, namely, a lack of Ag-specific PCs in the BM despite normal GC reaction and AFC production in the spleen post-immunization (Good-Jacobson et al., 2015). This was related to an inability of *c-Myb*-deficient PCs to migrate in response to Cxcl12. This loss-of-Cxcr4-function was not secondary to modulation of the membrane receptor, suggesting that *c-Myb* regulates responsiveness to Cxcl12 downstream of Cxcr4 and also plays a role in controlling the migration of PCs from secondary LOs to the BM. Combined with our findings, these results suggest that both increased and decreased Cxcr4-mediated signaling have similar effects on the trafficking of Ag-specific PCs between secondary LOs and the BM. Together they indicate that fine-tuning of Cxcr4 signaling is critical for the production of Ag-specific PCs in secondary LOs during a TD response and subsequently for their egress and homing to the BM and for the establishment of a stable resident PC pool for long-term protective humoral immunity.

Our observations are directly relevant to WS patients. Hypogammaglobulinemia constitutes a variable feature of WS with moderate deficiency of Igs seen in some but not all patients. They exhibit efficient primary responses following immune challenges, but their serum Ag-specific Ab titers appear to decline rapidly (Gulino et al., 2004; Handisurya et al., 2010;

Mc Guire et al., 2010; Tassone et al., 2009). For instance, in one study patients immunized with tetanus toxoid produce normal amounts of specific Abs 10 weeks after immunization, but no specific Ab was detectable at 1 year. This mirrors the phenotype of the *Cxcr4*⁺¹⁰¹³ mice, and our data would suggest that this reflects a defect in long-lived PC response and needs to be taken into account in managing this group of patients.

EXPERIMENTAL PROCEDURES

Mice and Immunization

Mice were immunized with 100 μ g of either OVA adjuvanted with SAS (Sigma-Aldrich) or 4-hydroxy-3-nitrophenylacetyl-keyhole limpet hemocyanine (NP-KLH) (Biosearch Technologies) adjuvanted with Alum (Thermo Scientific). Blood, spleen, BM, and inguinal LNs were harvested at the indicated time points and single-cell suspension were prepared. All experiments were conducted in compliance with the European Union guide for the care and use of laboratory animals and has been reviewed and approved by an appropriate institutional review committee (C2EA-26, Animal Care and Use Committee, Villejuif, France).

In Vitro Functional Assays

For apoptosis assays, splenocytes were stimulated with a F(ab')₂ goat anti-mouse IgM (Jackson ImmunoResearch) at 10 μ g/mL and/or Cxcl12 (R&D Systems) at 50 nM during 2 days at 37°C. For PC differentiation and qRT-PCR, B cells were isolated from total splenocytes using a mouse B cell isolation kit (Miltenyi Biotec) and stimulated with 1 U/mL of IL-4 (Miltenyi) and 5 ng/mL IL-5 (Miltenyi) supplemented with 10 μ g/mL F(ab')₂ goat anti-mouse IgM and 80 ng/mL CD40L (PeproTech) and/or 50 nM Cxcl12 during 4 or 6 days at 37°C.

Flow Cytometry

Single-cell suspensions were stained using the Abs described in the supplemental experimental procedures. NP conjugated to phycoerythrin (PE) was from Biosearch Technologies. OVA-FITC conjugate was purchased from Invitrogen. For phosphoflow analyses, splenocytes were pre-incubated in RPMI only with or without 10 μ M of AMD3100 (Sigma) before being stimulated with 10 μ g/ml of F(ab')₂ goat anti-mouse IgM and/or 50 nM Cxcl12 during 5 min at 37°C.

qRT-PCR

qPCRs were performed on a Light Cycler instrument (LC480, Roche Diagnostics) with the LightCycler 480 SYBR Green detection kit (Roche Diagnostics) or TaqMan chemistry (Applied Biosystems) using the primers listed in the supplemental experimental procedures. β -actin (*Actb*) was used as the reference standard for normalization, except for *Il-6* and *Trail* (normalized with *Gapdh*), and relative quantification of fold differences in mRNA expression was determined by the comparative delta-delta-ct ($2^{-\Delta\Delta CT}$) method.

Immunofluorescence

LNs and spleens cryosections were stained with different combinations of Abs detailed in the supplemental experimental procedures. Slides were scanned using a NanoZoomer Digital Pathology system using 2 \times , 10 \times , or 30 \times objective lenses with numerical aperture 0.75 (Hamamatsu Photonic).

ELISA and ELISpot

Serum anti-OVA IgG1 or anti-NP IgG1 titers were determined by ELISA, as previously described (Natt and Espéli, 2015). In differentiation assays, culture supernatants were incubated on wells pre-coated with 5 μ g/ml of goat anti-mouse IgM (Jackson ImmunoResearch) and saturated and then incubated with peroxidase-conjugated goat anti-mouse IgM (Southern Biotech). Enumeration of OVA- and NP-specific AFCs was performed by ELISpot assays from 5×10^5 inguinal LN cells or 1×10^5 spleen or BM cells per well, respectively, as previously described (Espéli et al., 2012; Pelletier et al., 2010).

Statistical Analyses

Data are expressed as means \pm SEM. The statistical significance between groups was evaluated using the two-tailed Student's *t* test (phosphoflow analyses) or the two-tailed unpaired Mann-Whitney non-parametric test for all other experiments (Prism software, GraphPad).

SUPPLEMENTAL INFORMATION

Supplemental Information includes Supplemental Experimental Procedures and five figures and can be found with this article online at <http://dx.doi.org/10.1016/j.celrep.2016.08.068>.

AUTHOR CONTRIBUTIONS

Conceptualization, M.E. and K.B.; Methodology, N.F., M.E., and K.B.; Formal Analysis: V.B., J.N., C.F., N.A., M.E., and K.B.; Investigation, V.B., J.N., C.F., N.A., A.S., P.H., F.G., M.E., and K.B. Writing – Original Draft, M.E. and K.B.; Writing – Review and Editing, V.B., J.N., C.F., N.A., and N.F.; Visualization, J.N., C.F., N.A., M.E., and K.B.; Supervision: M.E. and K.B.; Funding Acquisition: N.F., M.E., and K.B. M.E. and K.B. contributed equally to this study.

ACKNOWLEDGMENTS

We thank M.-L. Akinin and Dr. H. Gary (IPSIT, Facility PLAIMMO, Clamart) for their technical assistance. The study was supported by ANR grant 2010-JCJC-110401 to K.B., by a Junior Team Leader starting grant from the Laboratory of Excellence in Research on Medication and Innovative Therapeutics (LabEx LERMIT) and an ANR @RAction starting grant (ANR-14-ACHN-0008) to M.E., and by the Conseil Régional Midi-Pyrénées, Institut National contre le Cancer (INCa, PLBIO10-195 and INCA-6530) and FP7-MC-IRG-256471 to N.F. V.B., J.N., C.F., N.A., F.G., M.E., and K.B. are members of the LabEx LERMIT supported by ANR grant ANR-10-LABX-33 under the program Investissements d'Avenir ANR-11-IDEX-0003-01. V.B. was supported by fellowships from the French Ministry for education and the Fondation pour la Recherche Médicale (FRM). J.N. was a PhD fellow from the LabEx LERMIT. C.F. was supported by the DIM Biotherapies and the Société Française d'Hématologie (SFH). N.A. was supported by a fellowship from the French Ministry for education. A.S. was supported by la Ligue Nationale Contre le Cancer. We are grateful to Dr. S. Flint (University of Cambridge) for critical reading and editing of the manuscript and Dr. A. Bonaud (INSERM UMR_S996, Clamart) for her input and technical help.

Received: February 17, 2016

Revised: July 7, 2016

Accepted: August 19, 2016

Published: September 27, 2016

REFERENCES

Allen, C.D., Ansel, K.M., Low, C., Lesley, R., Tamamura, H., Fujii, N., and Cyster, J.G. (2004). Germinal center dark and light zone organization is mediated by CXCR4 and CXCR5. *Nat. Immunol.* *5*, 943–952.

Balabanian, K., Lagane, B., Pablos, J.L., Laurent, L., Planchenault, T., Verola, O., Lebbe, C., Kerob, D., Dupuy, A., Hermine, O., et al. (2005). WHIM syndromes with different genetic anomalies are accounted for by impaired CXCR4 desensitization to CXCL12. *Blood* *105*, 2449–2457.

Balabanian, K., Brotin, E., Biajoux, V., Bouchet-Delbos, L., Lainey, E., Fenneteau, O., Bonnet, D., Fiette, L., Emilie, D., and Bachelier, F. (2012). Proper desensitization of CXCR4 is required for lymphocyte development and peripheral compartmentalization in mice. *Blood* *119*, 5722–5730.

Bannard, O., Horton, R.M., Allen, C.D., An, J., Nagasawa, T., and Cyster, J.G. (2013). Germinal center centroblasts transition to a centrocyte phenotype according to a timed program and depend on the dark zone for effective selection. *Immunity* *39*, 912–924.

Beck, T.C., Gomes, A.C., Cyster, J.G., and Pereira, J.P. (2014). CXCR4 and a cell-extrinsic mechanism control immature B lymphocyte egress from bone marrow. *J. Exp. Med.* *211*, 2567–2581.

Calamito, M., Juntilla, M.M., Thomas, M., Northrup, D.L., Rathmell, J., Birnbaum, M.J., Koretzky, G., and Allman, D. (2010). Akt1 and Akt2 promote peripheral B-cell maturation and survival. *Blood* *115*, 4043–4050.

Campbell, K.S. (1999). Signal transduction from the B cell antigen-receptor. *Curr. Opin. Immunol.* *11*, 256–264.

Chu, V.T., Fröhlich, A., Steinhauser, G., Scheel, T., Roch, T., Fillatreau, S., Lee, J.J., Löhning, M., and Berek, C. (2011). Eosinophils are required for the maintenance of plasma cells in the bone marrow. *Nat. Immunol.* *12*, 151–159.

Dotta, L., Tassone, L., and Badolato, R. (2011). Clinical and genetic features of Warts, Hypogammaglobulinemia, Infections and Myelokathexis (WHIM) syndrome. *Curr. Mol. Med.* *11*, 317–325.

Espéli, M., Clatworthy, M.R., Bökers, S., Lawlor, K.E., Cutler, A.J., Köntgen, F., Lyons, P.A., and Smith, K.G. (2012). Analysis of a wild mouse promoter variant reveals a novel role for Fc γ R1b in the control of the germinal center and autoimmunity. *J. Exp. Med.* *209*, 2307–2319.

Gitlin, A.D., Shulman, Z., and Nussenzweig, M.C. (2014). Clonal selection in the germinal centre by regulated proliferation and hypermutation. *Nature* *509*, 637–640.

Gitlin, A.D., Mayer, C.T., Oliveira, T.Y., Shulman, Z., Jones, M.J., Koren, A., and Nussenzweig, M.C. (2015). HUMORAL IMMUNITY. T cell help controls the speed of the cell cycle in germinal center B cells. *Science* *349*, 643–646.

Good-Jacobson, K.L., O'Donnell, K., Belz, G.T., Nutt, S.L., and Tarlinton, D.M. (2015). c-Myb is required for plasma cell migration to bone marrow after immunization or infection. *J. Exp. Med.* *212*, 1001–1009.

Guinamard, R., Signoret, N., Ishiai, M., Marsh, M., Kurosaki, T., and Ravetch, J.V. (1999). B cell antigen receptor engagement inhibits stromal cell-derived factor (SDF)-1 α chemotaxis and promotes protein kinase C (PKC)-induced internalization of CXCR4. *J. Exp. Med.* *189*, 1461–1466.

Gulino, A.V., Moratto, D., Sozzani, S., Cavadini, P., Otero, K., Tassone, L., Imberti, L., Pirovano, S., Notarangelo, L.D., Soresina, R., et al. (2004). Altered leukocyte response to CXCL12 in patients with warts hypogammaglobulinemia, infections, myelokathexis (WHIM) syndrome. *Blood* *104*, 444–452.

Handisurya, A., Schellenbacher, C., Reininger, B., Koszik, F., Vyhnanek, P., Heitger, A., Kirnbauer, R., and Förster-Waldl, E. (2010). A quadrivalent HPV vaccine induces humoral and cellular immune responses in WHIM immunodeficiency syndrome. *Vaccine* *28*, 4837–4841.

Hargreaves, D.C., Hyman, P.L., Lu, T.T., Ngo, V.N., Bidgol, A., Suzuki, G., Zou, Y.R., Littman, D.R., and Cyster, J.G. (2001). A coordinated change in chemokine responsiveness guides plasma cell movements. *J. Exp. Med.* *194*, 45–56.

Hauser, A.E., Debes, G.F., Arce, S., Cassese, G., Hamann, A., Radbruch, A., and Manz, R.A. (2002). Chemotactic responsiveness toward ligands for CXCR3 and CXCR4 is regulated on plasma blasts during the time course of a memory immune response. *J. Immunol.* *169*, 1277–1282.

Hernandez, P.A., Gorlin, R.J., Lukens, J.N., Taniuchi, S., Bohinjec, J., Francois, F., Klotman, M.E., and Diaz, G.A. (2003). Mutations in the chemokine receptor gene CXCR4 are associated with WHIM syndrome, a combined immunodeficiency disease. *Nat. Genet.* *34*, 70–74.

Jacob, J., Kassir, R., and Kelsoe, G. (1991). In situ studies of the primary immune response to (4-hydroxy-3-nitrophenyl)acetyl. I. The architecture and dynamics of responding cell populations. *J. Exp. Med.* *173*, 1165–1175.

Kallies, A., Hasbold, J., Tarlinton, D.M., Dietrich, W., Corcoran, L.M., Hodgkin, P.D., and Nutt, S.L. (2004). Plasma cell ontogeny defined by quantitative changes in blimp-1 expression. *J. Exp. Med.* *200*, 967–977.

Kawai, T., and Malech, H.L. (2009). WHIM syndrome: congenital immune deficiency disease. *Curr. Opin. Hematol.* *16*, 20–26.

Kijowski, J., Baj-Krzyworzeka, M., Majka, M., Reza, R., Marquez, L.A., Christofidou-Solomidou, M., Janowska-Wieczorek, A., and Ratajczak, M.Z. (2001). The SDF-1-CXCR4 axis stimulates VEGF secretion and activates integrins but does not affect proliferation and survival in lymphohematopoietic cells. *Stem Cells* *19*, 453–466.

- Lagane, B., Chow, K.Y., Balabanian, K., Levoye, A., Harriague, J., Planchenault, T., Baleux, F., Gunera-Saad, N., Arenzana-Seisdedos, F., and Bachelier, F. (2008). CXCR4 dimerization and beta-arrestin-mediated signaling account for the enhanced chemotaxis to CXCL12 in WHIM syndrome. *Blood* 112, 34–44.
- Liu, Y.J., Zhang, J., Lane, P.J., Chan, E.Y., and MacLennan, I.C. (1991). Sites of specific B cell activation in primary and secondary responses to T cell-dependent and T cell-independent antigens. *Eur. J. Immunol.* 21, 2951–2962.
- Ma, Q., Jones, D., Borghesani, P.R., Segal, R.A., Nagasawa, T., Kishimoto, T., Bronson, R.T., and Springer, T.A. (1998). Impaired B-lymphopoiesis, myelopoiesis, and derailed cerebellar neuron migration in CXCR4- and SDF-1-deficient mice. *Proc. Natl. Acad. Sci. USA* 95, 9448–9453.
- Ma, Q., Jones, D., and Springer, T.A. (1999). The chemokine receptor CXCR4 is required for the retention of B lineage and granulocytic precursors within the bone marrow microenvironment. *Immunity* 10, 463–471.
- Mc Guire, P.J., Cunningham-Rundles, C., Ochs, H., and Diaz, G.A. (2010). Oligoclonality, impaired class switch and B-cell memory responses in WHIM syndrome. *Clin. Immunol.* 135, 412–421.
- Nakai, A., Hayano, Y., Furuta, F., Noda, M., and Suzuki, K. (2014). Control of lymphocyte egress from lymph nodes through β 2-adrenergic receptors. *J. Exp. Med.* 211, 2583–2598.
- Natt, J., and Espéil, M. (2015). Assessing T follicular helper cell function in vivo: antigen-specific B cell response to hapten and affinity maturation. *Methods Mol. Biol.* 1291, 87–101.
- Nie, Y., Waite, J., Brewer, F., Sunshine, M.J., Littman, D.R., and Zou, Y.R. (2004). The role of CXCR4 in maintaining peripheral B cell compartments and humoral immunity. *J. Exp. Med.* 200, 1145–1156.
- Ochsenbein, A.F., Pinschewer, D.D., Sierro, S., Horvath, E., Hengartner, H., and Zinkernagel, R.M. (2000). Protective long-term antibody memory by antigen-driven and T help-dependent differentiation of long-lived memory B cells to short-lived plasma cells independent of secondary lymphoid organs. *Proc. Natl. Acad. Sci. USA* 97, 13263–13268.
- Okada, T., Ngo, V.N., Ekland, E.H., Förster, R., Lipp, M., Littman, D.R., and Cyster, J.G. (2002). Chemokine requirements for B cell entry to lymph nodes and Peyer's patches. *J. Exp. Med.* 196, 65–75.
- Omori, S.A., Cato, M.H., Anzelon-Mills, A., Puri, K.D., Shapiro-Shelef, M., Calame, K., and Rickert, R.C. (2006). Regulation of class-switch recombination and plasma cell differentiation by phosphatidylinositol 3-kinase signaling. *Immunity* 25, 545–557.
- Pelletier, N., McHeyzer-Williams, L.J., Wong, K.A., Urich, E., Fazilleau, N., and McHeyzer-Williams, M.G. (2010). Plasma cells negatively regulate the follicular helper T cell program. *Nat. Immunol.* 11, 1110–1118.
- Pogue, S.L., Kurosaki, T., Bolen, J., and Herbst, R. (2000). B cell antigen receptor-induced activation of Akt promotes B cell survival and is dependent on Syk kinase. *J. Immunol.* 165, 1300–1306.
- Radbruch, A., Muehlinghaus, G., Luger, E.O., Inamine, A., Smith, K.G., Dörner, T., and Hiepe, F. (2006). Competence and competition: the challenge of becoming a long-lived plasma cell. *Nat. Rev. Immunol.* 6, 741–750.
- Rodda, L.B., Bannard, O., Ludewig, B., Nagasawa, T., and Cyster, J.G. (2015). Phenotypic and Morphological Properties of Germinal Center Dark Zone Cxcl12-Expressing Reticular Cells. *J. Immunol.* 195, 4781–4791.
- Sugiyama, T., Kohara, H., Noda, M., and Nagasawa, T. (2006). Maintenance of the hematopoietic stem cell pool by CXCL12-CXCR4 chemokine signaling in bone marrow stromal cell niches. *Immunity* 25, 977–988.
- Suzuki, H., Matsuda, S., Terauchi, Y., Fujiwara, M., Ohteki, T., Asano, T., Behrens, T.W., Kouro, T., Takatsu, K., Kadowaki, T., and Koyasu, S. (2003). PI3K and Btk differentially regulate B cell antigen receptor-mediated signal transduction. *Nat. Immunol.* 4, 280–286.
- Tachibana, K., Hirota, S., Iizasa, H., Yoshida, H., Kawabata, K., Kataoka, Y., Kitamura, Y., Matsushima, K., Yoshida, N., Nishikawa, S., et al. (1998). The chemokine receptor CXCR4 is essential for vascularization of the gastrointestinal tract. *Nature* 393, 591–594.
- Tassone, L., Notarangelo, L.D., Bonomi, V., Savoldi, G., Sensi, A., Soresina, A., Smith, C.I., Porta, F., Plebani, A., and Badolato, R. (2009). Clinical and genetic diagnosis of warts, hypogammaglobulinemia, infections, and myelokathexis syndrome in 10 patients. *J. Allergy Clin. Immunol.* 123, 1170–1173.
- Ursini-Siegel, J., Zhang, W., Altmeyer, A., Hatada, E.N., Do, R.K., Yagita, H., and Chen-Kiang, S. (2002). TRAIL/Apo-2 ligand induces primary plasma cell apoptosis. *J. Immunol.* 169, 5505–5513.
- Victoria, G.D., Schwickert, T.A., Fooksman, D.R., Kamphorst, A.O., Meyer-Hermann, M., Dustin, M.L., and Nussenzweig, M.C. (2010). Germinal center dynamics revealed by multiphoton microscopy with a photoactivatable fluorescent reporter. *Cell* 143, 592–605.
- Vinuesa, C.G., Tangye, S.G., Moser, B., and Mackay, C.R. (2005). Follicular B helper T cells in antibody responses and autoimmunity. *Nat. Rev. Immunol.* 5, 853–865.
- Winter, O., Moser, K., Mohr, E., Zotos, D., Kaminski, H., Szyska, M., Roth, K., Wong, D.M., Dame, C., Tarlinton, D.M., et al. (2010). Megakaryocytes constitute a functional component of a plasma cell niche in the bone marrow. *Blood* 116, 1867–1875.